New enaminone-based to the sesquiterpenic: TiCl4-catalyzed synthesis, spectral characterization, crystal structure, Hirshfeld surface analysis, DFT studies and cytotoxic activity

Abdoullah Bimoussa, Ali Oubella, Mouhi Eddine Hachim, My Youssef Ait Itto, Olivier Mentré, El Mostafa Ketatni, Lahoucine Bahsis, Hamid Morjani, Aziz Auhmani

New enaminone-based to the sesquiterpenic skeleton: $TiCl_4$-Catalyzed Synthesis, Spectral Characterization, Crystal Structure,Hirshfeld surface analysis, DFT studies, and cytotoxic activity

Abdoullah BIMOUSSA[1,] Ali OUBELLA[1,], Mouhi Eddine Hachim[7],My Youssef AIT ITTO[1], Olivier MENTRE[3],El Mostafa KETATNI[2],Lahoucine BAHSIS[4,5],Hamid MORJANI[6]andAziz AUHMANI[1,*]

[1-]Laboratory of Organic Synthesis and Physico-Molecular Chemistry, Department of Chemistry, Faculty of Sciences Semlalia, B.P. 2390, Marrakech 40001, Morocco.
[2-]Laboratory of Applied Spectro-Chemistry and the Environment, University Sultan MoulaySlimane, Faculty of Sciences and Technology, PO Box 523, Beni-Mellal, Morocco.
[3-]Univ. Lille, CNRS, Centrale Lille, ENSCL, Univ. Artois, UMR 8181 - UCCS-Catalysis and Solid Chemistry Unit, F-59000 Lille, France.
[4] Laboratoire de Chimie Analytique et Moléculaire, Faculté Polydisciplinaire, Université Cadi Ayyad, BP 4162, 46000 Safi, Morocco.
[5-]Laboratoire de Chimie de Coordination et d'Analytique,Département de Chimie, Faculté des Sciences d'El Jadida, Université Chouaïb Doukkali, B.P :20, El Jadida 24000, Morocco
[6]BioSpectroscopie Translationnelle, BioSpecT - EA7506, UFR de Pharmacie, Université de Reims Champagne-Ardenne, 51 Rue Cognacq Jay, 51096, Reims Cedex, France.
[7-]Équipe de modélisation moléculaire et de spectroscopie, Faculté des sciences, Université de ChouaïbDoukkali, El Jadida, Morocco.

Corresponding author:a.auhmani@uca.ac.ma,

Abstract

In this work, the compound **2** named ethyl (1,1-dichloro-1a,5,5,7-tetramethyl-8-oxo-1a,2,3,4,5,5a,8,9-octahydro-1H-benzo[a]cyclopropa[b][7]annulen-6-yl)glycinate ($C_{20}H_{29}C_{l2}NO_3$) was synthesized from the α,β-unsaturated sesquiterpenicketone**1** using the azido-Schmidt reaction catalyzed by titanium tetrachloride ($TiCl_4$). The structure of the newly synthesized enaminone **2** was fully identified on the basis of its HRMS, FT-IR, UV-Visible, NMR (^1H &^{13}C) spectral data, and X-ray crystallography. The compounds **1** and **2** were evaluated for their cytotoxic activity in four human cancer cell lines, fibrosarcoma (HT-1080), lung carcinoma (A-549), and breast (MCF-7 and MDA-MB-231). Data showed that compound **1** wasthe most activeagainst HT-1080 and A-549 cells with IC_{50} values between 13.28 and 16.41 µM.Thetheoretical Study Theory (DFT) was used to predict the molecular proprieties which lead to the highest potential of cytotoxic effect, in accordance to the experimental spectroscopic data.

Keywords: Sesquiterpene, Crystal structure, Hirshfeld surface analysis, DFT, Cytotoxicity, Spectroscopy.

1. Introduction

Today, the cancer is considered as major cause of morbidity and mortality worldwide. Thus, cancer is recognized to induce over 10 milliondeaths [1]. In spite of all efforts and progress in cancer research, cancer treatment still faces a lot of challenges, such as, the chemoresistance, non-selectivity, and several side effects of therapies, especially chemotherapy.Consequently, several works are currently carried out to develop new anticancer agents based on natural products with better safety profiles and improved selectivity against tumor cells [2-5].β-enaminones are key intermediates thathave widely used in medicinal chemistry. Such compounds are remarkable synthons for the synthesis of a wide variety of bioactive molecules containing heterocycles and naturally occurring alkaloids [6-7], because of lipophilicity and extreme sensitivity to minor changes in the structure of the N-C=C-C=O backbone. On another note, it has also been reported that enaminone based products show antibacterial activity [8] and have anticonvulsant [9] and antitumor properties [10].The conjugated system of enaminone function is considered a functional group in drugs [11].In addition, the sesquiterpenestheir part, are considered a class of natural products with a broad spectrum of therapeutic potentials for cancer treatment [12-14].In terms of stability, the enaminones derived from β-carbonyl compounds are quite stable, probably due to keto-enol and imine-enamine tautomeric equilibria (**Scheme 1**).

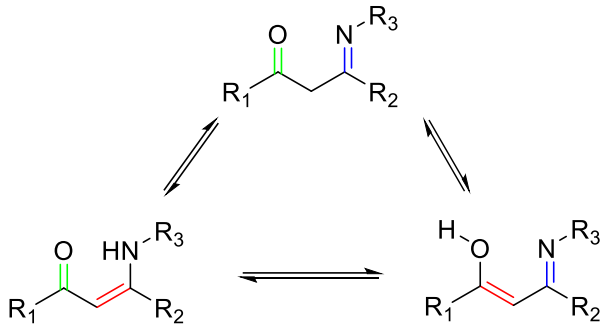

Scheme 1. Tautomeric equilibria of enaminones.

Due to their rich applications, many synthesis approaches to these compounds have been developed.The most popular route for the synthesis of β-enaminones is the condensation of β-dicarbonyl compounds with amines, or activation of methylene ketones by dialkylamino dimethyl acetals [15]. Various modified synthetic pathways have been reported in literature for the synthesis of β-enaminones using Lewis acids, inorganic acids, ionic liquids, and transition metal catalysts [16]. In addition, other procedures of synthesis were used, such as, microwave [17] and ultrasound irradiations [18].However, α,β-unsaturated ketones react with alkyl-azides upon treatment with Lewis acids via 1,3-dipolar cycloaddition reactions leading to the formation products of expansion resulting from the intermolecular or intramolecular reaction (Azido-Schmidt) [19-20].On the other hand, the catalyst plays an important role in the preparation of 1,

2, 3-triazoline, this later facilitates the conversion to enamine or lactam analogues [21-22].The direct condensation of amines with 1,3-diketone by refluxing in the presence of various catalysts also gives two isomeric enaminones [23-27].According to this bibliographic overview and in continuation of our efforts in the valorization of sesquiterpenes by the synthesis of new compounds [28], we report a simple and selective method for the synthesis of an enaminone based on himachalene using 1,3-dipolar reaction of azide-alkyl with α,β-unsaturated ketone catalyzed by $TiCl_4$.Both spectroscopic and theoretical studies had been undertaken using DFT/B3LYPmethod at 6-31+G(d,p) level. Also, the local reactivity indexes were carried out to investigate the plausible mechanisms for the regioselective synthesis of the compound **2**. Finally, the evaluation of the cytotoxic activity of the newly prepared enaminone and its support is also reported.

2. Experimental

Materials and Physical measurements

All chemicals were used as obtained from commercial sources(Aldrich and Acros). Melting point (m.p) was determined using a capillary apparatus and are inaccurate. Analytical thin-layer chromatography (TLC) was performed on plates precoated with E.Merck silica gel 60 F254 to a thickness of 0.25 mm. HRMS was obtained on a Q-TOF micromass spectrometer. ^{1}H and ^{13}C NMR spectra were recorded in $CDCl_3$ with 300 MHz Bruker Avance III spectrometer with a BBFO + probe. Chemical shifts (δ) are expressed in parts per million (ppm). They were recorded relative to solvent $CDCl_3$ signal (7.26 ppm and 77.16 ppm).FT-IR spectra were recorded on Bruker Vertex 70 spectrometer using a potassium bromide disc in the frequency range 4000-400 cm^{-1}.UV–Visible spectrum was obtained with a PASTEL UVILINE 9100/9400spectrophotometer, using a solution in DMF in the range of 200–800 nm.It's worthy to mention here that the compound **2** was isolated and identified according to the reported method [29].

2.1. General procedure for the preparation of enaminone2

To a stirred solution of α,β-unsaturated ketone (300 mg, 1.0 mmol) and alkyl azide (2.0 mmol) in CH_2Cl_2 (12 mL) was added per portion (during 30min) at 0 °C of $TiCl_4$ catalyst (1.0 mmol). After 18 hours stirring (the reaction was monitored by TLC) at room temperature, the layers were separated and the aqueous layer was extracted with CH_2Cl_2 (3 × 10 mL). The combined organic extracts were dried over anhydrous Na_2SO_4 and evaporated in vacuo. The residue was purified by column chromatography using hexane/ethylacetate mixture as eluent and recrystallized from mixture of ethanol-DMF.

Ethyl (1,1-dichloro-1a,5,5,7-tetramethyl-8-oxodecahydro-1Hbenzo[a]cyclopropa[b][7]annulen-6-yl) glycinate **2**.

Colorless crystals; yield 72%; m.p: 121-122 °C; HRMS (TOF-MS ES+) (m/z)$[M+H]^+$ calculated for $C_{20}H_{29}Cl_2NO_3$: 401.1524;found:401.1498.UV (λ_{nm}, in DMF):λ_1=269 nm,λ_2=342 nm.FT-IR (KBr disk, $\upsilon_{max,}$ cm^{-1}): 3423 (N-H); 2930 (C-H); 1716 (C=O); 1448 (C–O) (ester);1372 (C=C); 710.04 (C-Cl).^{1} H NMR δ (ppm): 0.77(3H, s); 1.05 (3H, s); 1.12 (3H, s); 1.81 (3H, s); 1.24 (3H, t, *J* = 7.14Hz);1.18-1.45 (2H, m); 1.50-1.79 (5H, m);2.60 (2H, AB system, *J* = 18.80Hz); 4.01 (2H, dd, J_1= 11 Hz, J_2= 2.2Hz); 4.2 (2H, q, *J* = 7.15 Hz); 5.01 (1H, s).^{13}C NMR δ (ppm): 8.07 (C17); 14.09 (C13); 15.39 (C10); 27.65 (C12); 30.06 (C11); 44.95 (C5a); 20.64 (C3); 29.64 (C4); 34.53 (C2); 35.78 (C9); 25.03 (C5); 32.59 (C1a);39.35 (C9a); 45.99 (C14);62.01 (C16);77.08 (C1); 110.54 (C7);160.35 (C6);169.22 (C15);193.22 (C8).

2.2. Structure solution and refinement

Reflection intensities for the enaminone ($C_{20}H_{29}Cl_2NO_3$)**2** was measured on Bruker DUO APEX-II CCD diffractometer and Mo$K_\alpha$graphite-monochromated radiation (= 0.71073 Å) at room temperature 299K. SAINT$^+$ 6.02 program was used for extraction and integration of diffraction intensities and SADABS program was carried out for correction of absorption effect [30]. The structures were solved by direct methods using SHELXTL-2014/5 [31] and refined (by weighted full matrix least-square on F^2 technics) to convergence using the SHELXL-2018/3 program [32]. All non-hydrogen atoms were refined anisotropically. All hydrogen atoms were fixed geometrically and were allowed refined using a riding model with U_{iso}(H) = 1.2–1.5U_{eq}(C). The absolute configuration was reliably determined based on the value of the Flack parameter [-0.005(19)].Details on the crystallographic studies, as well as atomic displacement parameters, are given as Supporting Information in the form of cif files. The plot of the molecule and the three-dimensional drawing of the crystal structure are obtained using the Diamond programs [33].

2.3.Hirshfeld surface and 2D fingerprint plots.

The Hirshfeld surfaces calculated for enaminone provide additional information on the distinctive contributions made to the molecular packing. Thus, a Hirshfeld surface analysis [34] and the associated two-dimensional fingerprint plots [35] were performed using CrystalExplorer17.5 [36] to figure out the normalized contact distance (d_{norm}), which depends on contact distances to the closest atoms outside (d_e) and inside (d_i) the surface. The molecular HS were performed using a standard (high) surface resolution with the three-dimensional surfaces mapped over a fixed color scale of -0.4586 to 1.4592a.u. The electrostatic potential were generated using *TONTO* implanted in Crystal Explorer 17.5 with the 6-31g(d,p) basis set at the Hartree–Fock level of theory, energy in the range -0.1010 to +0.1299 a.u.

2.4. Quantum chemical calculations

The quantum chemical calculation was donethrough DFT and TD-DFT calculations using Gaussian 09 version D.01. All geometry optimization was performed employing the hybrid B3LYP functional and 6-31G(d) basis set[37] and all obtained frequencies are positive, proving that all structure correspond to minimum energy.The implicit solvent effect was considered employing the integral equation formalism polarizable continuum model (CPCM) [38].

2.5. Cell culture

The human fibrosarcoma cell line HT-1080 (CCL 121) was purchased from Sigma Aldrich (ECACC collection, SaintQuentinFallavier, France). The human breast adenocarcinoma MCF-7 (HTB-22) and MDA-MB-231(HTB-26); and lung carcinoma A549 (CCL-185) cell lines were purchased from the American Type Culture Collection (ATCC). Cells were cultured in MEM (HT-1080) and DMEM (A549, MCF-7 and MDA-MB-231) with Earle salts and Glutamax I (Invitrogen, Cergy-Pontoise, France) supplemented with 10% fetal bovine serum, (Invitrogen) and 1% penicillin-streptomycin (Invitrogen). Cultures were maintained at 37 °C in a humidified atmosphere containing 5% CO_2 (v/v). Cells were routinely passaged at preconfluency using 0.05% trypsin, 0.53 mM EDTA (Invitrogen) and screened for the absence of mycoplasma using PCR method.

2.6 Cytotoxicity Assay

Cytotoxicity of the synthesized compounds was assessed by the CellTiter 96® Cell Proliferation Assay (MTT) (Promega, Charbonnieres les Bain, France). Briefly, the cells were plated at a density of 2500 cells/well in 96-well plates with 100 µL culture medium, containing different concentrations of the previously cited molecules (6.25, 12.5, 25, 50 and 100 µM). After 24 hours, 15 µL of MTT dye solution was added in each well. The plates were further incubated for 4 hours. Then, 100 µL of the solubilization/stop solution was added into each well and the plate was incubated 1hour at room temperature. The optical density of each well was measured at 570 nm using the microplatereader revelation 96-well multiscanner (Dynex Technologies, Chantilly, VA). Data were represented as a percentage of cell growth relative to untreated cells. The IC_{50} was defined as the drug concentration required for inhibition of cell growth by 50%.

3. Results and discussion

3.1. Hemisynthesis

Generally, the literature refers extensively to different classical and catalytic methods for the preparation of enaminones [39-40]. Aiming at the synthesis of a new enaminone with sesquiterpenic skeleton, we have examined the 1,3-dipolar cycloaddition reactionof α, β-unsaturated ketone **1** (used as dipolarophile) with a stoichiometric quantity of $TiCl_4$ catalyst (used as Lewis acid) and a double stoichiometric amount of ethyl azide acetate (used as 1,3-dipole).The reaction was performed, at room temperature, in dichloromethane as solvent to

produce the corresponding enaminone **2** in a good yield (72%) (**Scheme 2)**. It's worthy to mention here that the reaction also was catalyzed by several catalysts, such as, CuI, SiO_2 and $AlCl_3$, but no reaction was observed.

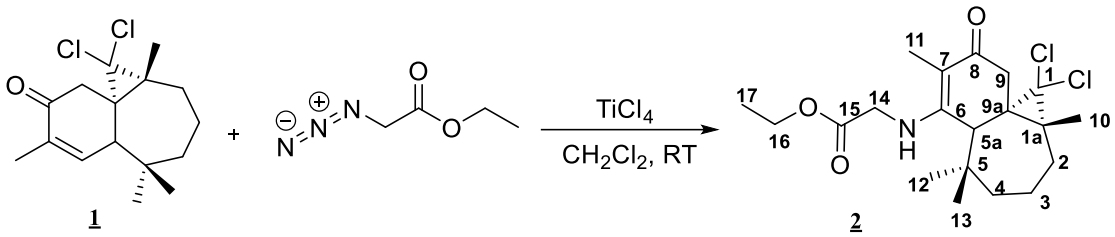

Scheme 2: Reaction of α,β-unsaturatedketone **1**with ethyl azido-acetate

It should be pointed out that the NMR spectrum of the product found shows no resonances of CH(sp^3) of 1,2,3-triazole nucleus **A**, however, its FT-IR and NMR spectra clearly show a signal characterizing the function amine (H-N) at (NMR: δ^1H 5.01 ppm) and (FT-IR: υ_{max}3423 cm^{-1}). In addition, its HRMS spectrum show the corresponding pseudo-molecular ion $[M+H]^+$ at m/z = 401.1498, consistent with the enaminone molecular formula (**2**: $C_{20}H_{29}Cl_2NO_3$) and not with the molecular formula of 1,2,3-triazole **A**. In the light of all these spectral evidences, we can state that the 1,2,3-triazole **A** is an unstable compound and intermediate for the preparation of enaminone **2** following the mechanism proposed in **Scheme3**.

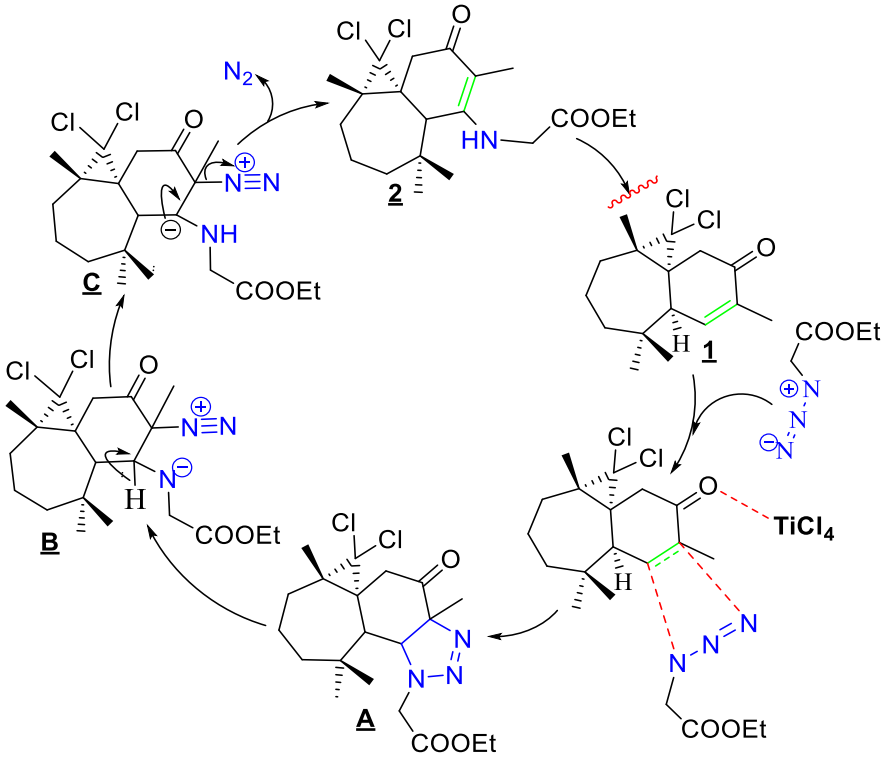

Scheme 3: The proposed mechanism of the formation of compound **2**

On the basis of control experiments and spectroscopic studies as well as the reaction condition using only lewis acid ($TiCl_4$), a probable mechanism of the reaction of the azide alkyl with himachalene ketone **1** has been proposed (**Scheme 3**). Firstly, the initial support **1** may get activated in the carbonyl group in the presence of $TiCl_4$ by forming an organo-metallic complex

to facilitate the condensation of azide via 1,3-dipolar cycloaddition mechanism, which produces intermediate **A** (1,2,3-triazole). Subsequently, the 1,2,3-triazole then transforms into the charged species of zwitterionic type **B** via a cleavage between the N-N. The proton released during the formation of intermediate **C** is able to emigrate to nitrogen atom, which to enables the departure of N_2 and the formation of product **2**.

3.2 Spectral Characterization

3.2.1 ^{1}H NMR and ^{13}C NMR spectrum analysis

The chemical structure of the newly prepared enaminone **2** was fully confirmed by its NMR (^{1}H &^{13}C) spectral data which mainly reveal the disappearance of the double bond HC=C (δ^{1}H 6.25 ppm) characteristic of product **1**. Whereas, instead we note H_3C17 (one triplet δ^{1}H 1.24 ppm J = 7.14Hz; δ^{13}C 8.07ppm) and H_2C16 (one quadruplet δ^{1}H 4.20 ppm J = 7.15Hz; δ^{13}C 62.01 ppm) resonances.In the same spectra, we still note, a doublet of doublets at (δ ^{1}H 4.01 ppm J_1 = 11, J_2 = 2.2 Hz; δ ^{13}C 35.78 ppm) corresponding to the methylene (N-CH_2) proton at position 1', the second towards δ ^{1}H 5.01 ppm assigned to NH, and the third, such as, methylene (H_2C9) appear as an AB system at (δ ^{1}H 2.60 ppm, J = 18.80Hz; δ ^{13}C 35.78 ppm).Indeed, in its ^{13}C NMR spectrum, we also notice the appearance of a new signal due to the ester group (C=O) at 169.22ppm, also the moiety (C=C) emanating from the cyclohexene at 110.54ppm, and at 160.35 ppm. In terms theoretical analysis, ^{1}H and ^{13}C NMR chemical shifts of compound **2** were carried out at the B3LYP/6-31G(d,p) using GIAO approach in solvent phase. The calculations were performed in $CDCl_3$ solvent by using C-PCM formalism, and the selected shifts were compared with the experimental values as illustrated in **Table 1**.

Table 1. Selected experimental and theoretical ^{1}H and ^{13}C NMR shifts (ppm) of product**2**.

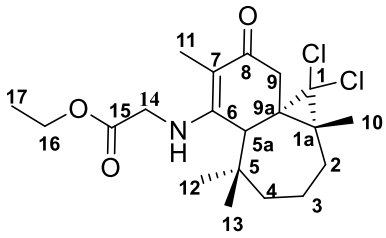

^{1}H NMR chemical shifts (ppm)			^{13}C NMR chemical shifts (ppm)		
Atoms	Experimental ($CDCl_3$)	Calculated DFT/B3LYP (ppm)	Atoms	Experimental ($CDCl_3$)	Calculated DFT/B3LYP (ppm)
H-14	4.01	4.18	C14	45.99	37.99
H-16	4.2	4.31	C16	62.01	54.76
H-17	1.24	1.27	C17	8.07	5.58
H-9	2.6	2.36	C9	35.78	29.95
H-5a	2.43	2.28	C5a	44.95	44.03
N-H	5.01	4.99	C2'	169.22	155.87
			C6	160.35	147.40

	C7	110.54	97.67
	C8	193.22	174.54

According to **Table 1**, we can see that, the highest chemical shift value of C8 atom and the lowest of C17 were observed at 193.22 ppm (experimental) and 174.54 ppm (theoretical) for C8 atom, and 8.07ppm (experimental) and 5.58 ppm (theoretical) for C17 atom.In this study, and as expected, ester group C15 carbon atom, and alkene (C6 & C7) were recorded at 169.22 ppm (experimental), 155.87 ppm (calculated) for C15, also, 110-160 ppm (experimental), 90-150 ppm (calculated) for C7 and C6. But, the carbon atom C14, attached to the N atom, has slightly bigger chemical shift than the other carbon atoms of the same nature, probably came from of that nitrogen atom at which its alpha position creating an electronegative effect influenced the resonance value, of which its experimental value is 45.99 ppm and that calculated is 37.99 ppm. On the other hand, the correlation coefficients R^2 of 98.79% and 99.84% for the selected ^{1}H and ^{13}C NMR chemical shifts, respectively (**Fig. 1**). The conclusion to be drawn concerning the comparability between the experimental and the theoretical is that experimental NMR data are consistent with the computed values from the optimized structure of **2**.

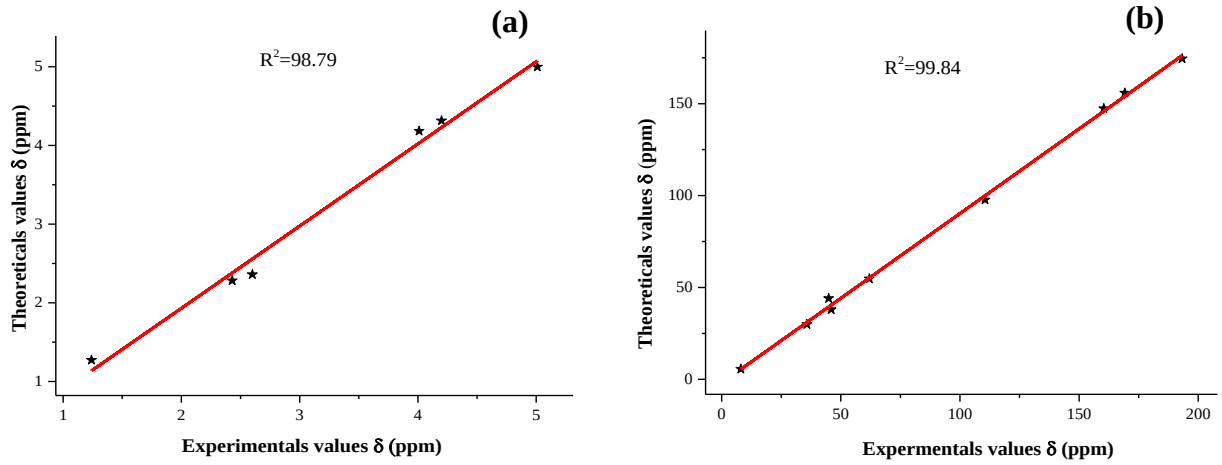

Fig. 1. Correlation curves between the predicted and experimental ^{1}H NMR (a) and ^{13}C NMR (b) chemical shifts for product **2**.

3.2.2 IR Spectral analysis

Subsequently, FT-IR spectral study of title compound was carried out. The structure of compound **2** was confirmed according to its IR spectral data, where was indicated the existence of the band at ν_{max} = 3423 cm^{-1} that corresponded to the secondary amine (NH), a band of carbonyl group (ketone) at 1716cm^{-1}, and the strong band characteristic of the ester function at 1448cm^{-1}.In addition, the scaled harmonic vibrational frequencies of compound **2** were calculated from the optimized structure with DFT/B3LYP using 6-31G(d,p) basis set at room temperature in the region between 400 and 4000 cm^{-1}. The experimental and theoretical

spectrums plotted on the transmittance (%) against the wave number (cm^{-1}) are shown in **Figure 2**.

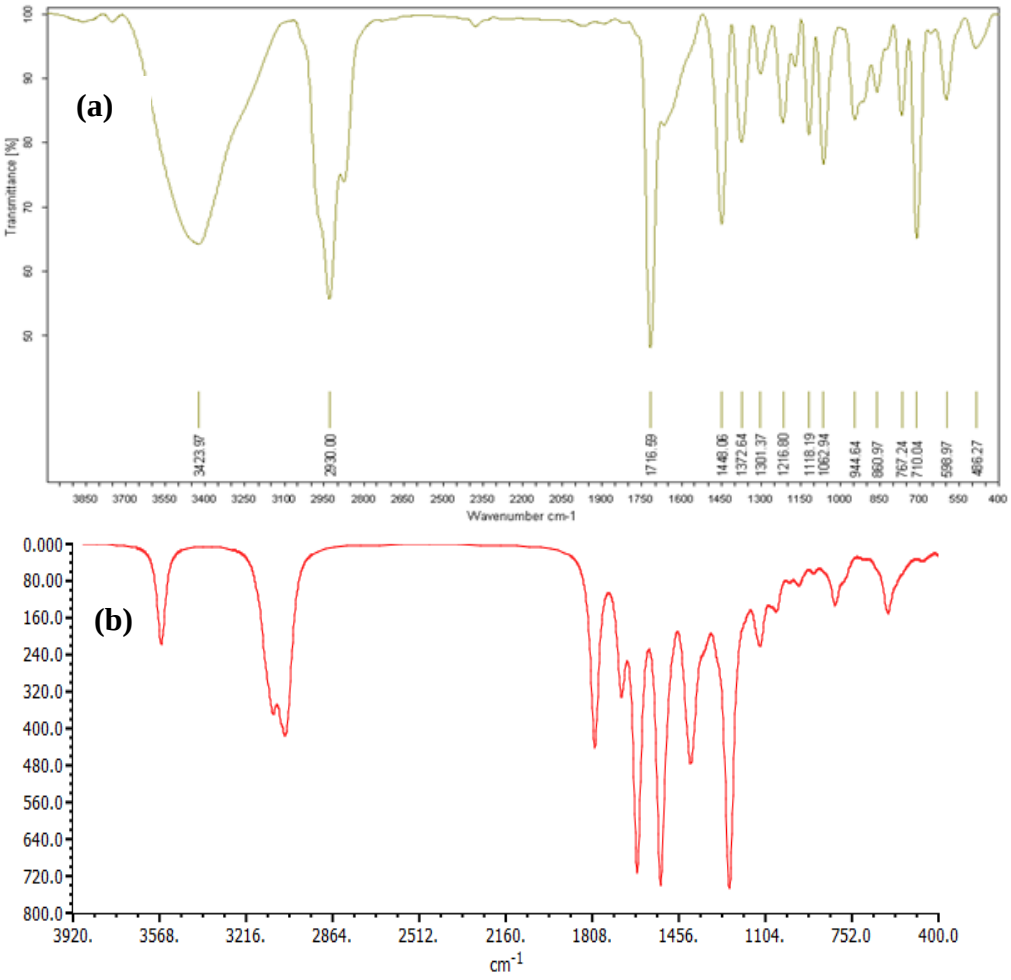

Fig.2. Experimental FT-IR spectrum (a) and theoretical IR spectrum of the title compound (b).

The calculated frequencies were compared with the observed values and the results found are grouped in **Table 2**.

Table 2. Comparison of the experimental and theoretical vibrational spectra analysis of the compound **2**.

Assignment Experimental FT-IR Calculated (cm^{-1}) (cm^{-1}) with KBrB3LYP/6-31G(d,p)		
$\upsilon(C=O)_{Ketone}$	1716	1693
$\upsilon(C-O)_{Ester}$	1448	1434
$\upsilon(C=C)$	2930	3036
$\upsilon(N-H)$	3423	3564
$\upsilon(C=C)$ 1372	1371	
$\upsilon(C-Cl)$710	711	

The experimental C=O stretch band at 1716 cm^{-1} for the ketone and 1448 cm^{-1} for ester are in accordance with results from previous report[41-42], and it were found to be in good agreement with the computed values at 1693 cm^{-1} and 1434 cm^{-1},respectively.N-H stretching absorption

band, as can be seen in the **Table 2**, this band is stated 3423 and 3564 cm^{-1} experimentally and theoretically, respectively.

3.2.3 UV-Vis Spectral Analysis

UV-Vis spectral analysis of the compound **2** was realized with TD-DFT/B3LYP/6-31G(d,p) in DMF-Dimethylformamide solvent. The absorption wavelengths are recorded at 269, 342 nm and 249, 301nm as spectral results and theoretical predictions, respectively. The maximum value (342 nm) is related to the n→π* transition of around enaminone moiety probably due to the presence of carbon-nitrogen simple bond. Moreover, the experimental wavelength of 269nm can be generated from π→π* transitions of cyclohexenone ring. All experimental and theoretical data, such as, potential transitions, wavelengths (λ,nm), excitation energies (eV) and oscillator strengths (f) are represented in **Table 3**. Also, the experimental UV-Vis spectrum is shown in **Figure 3**.

Table 3. The experimental and theoretical UV-Vis spectra parameters of the compound **2**

Experimental Wavelength (in DMF) λmax (nm)	Calculated with TD-DFT/B3LYP/6-31G(d,p) (in DMF)				
	Wavelength λmax (nm)	Excitation Energy (eV)	Oscillator Strength f	Probable Orbital Transition	Assignment
342	301.57	4.1113	0.4719	HOMO →LUMO (67%) HOMO-1→LUMO (22%)	n→π*
269	249.77	4.9639	0.0084	HOMO-2→LUMO(69%) HOMO-3→LUMO(12%)	π→π*

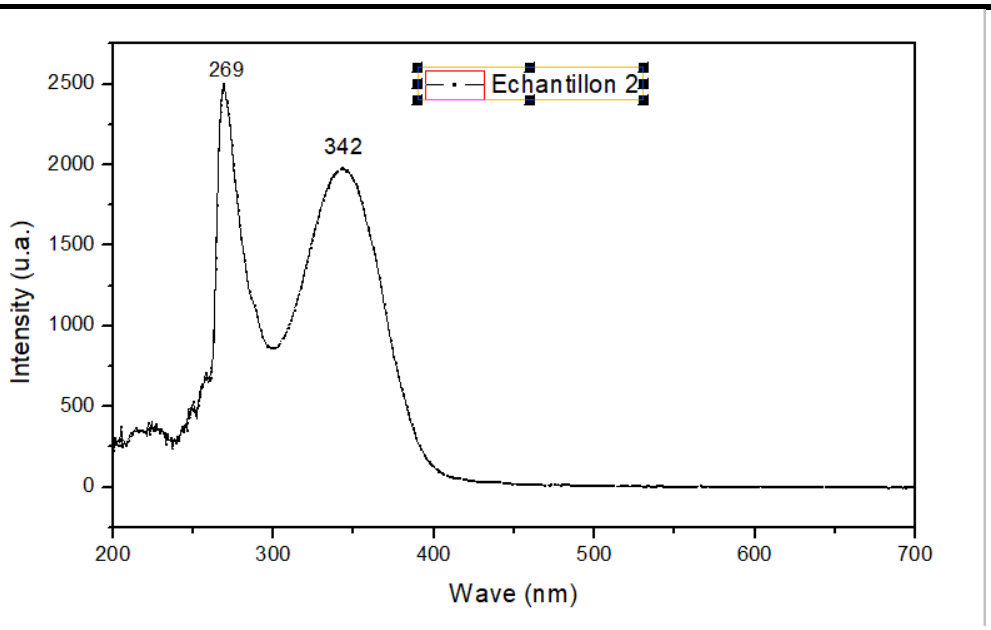

Fig. 3. Electronic absorption spectra of compound **2** (25 °C, DMF)

3.3 Crystal structure description of compound 2

To ascertain all these structural evidences resulting from these spectroscopic techniques. This prompted us to carry out X-ray analyses on single crystals of product**2**, which provide

indisputable proofs of the assigned structure and allow us to state with certainty that the compound obtained via 1,3-dipolar cycloaddition between azide and the compound **1** is the enaminone **2**. Enaminone was crystallized from mixture of ethanol-DMF to give very crystals suitable for single crystal X-ray measurements. The title compound crystallizes in the orthorhombic system with non centrosymetric space group $P2_12_12_1$. The structural diagrams of the crystal structure determined in this study are shown in Scheme 2, and the crystallographic asymmetric-unit contents are shown in **Fig. 4**. Crystal data, data collection and structure refinement details are summarized in **Table 4**. The selected bond distances and angles are reported in **Table 5**. The structure of the title compound is built up from a cycloheptane ring (C1a/C2–C9a), which is fused to a cyclohexene ring (C5a/C6–C9a), and a cyclopropane ring (C1–C2-C9a). The cyclohexene ring is substituted by an amino-α- ester function**.**

Table 4: Crystal Data, Summary of Intensity Data Collection and Structure Refinement of **2**

Empirical formula	$C_{20}H_{29}Cl_2NO_3$
Formula weight	402.34
Temperature	298(2)
Wavelength	0.71073 Å
Crystal system, space group	orthorhombic, $P2_12_12_1$
a, b, c (Å)	9.4166(9), 11.4499(10), 19.3375(18)
Volume (A^3)	2085.0(3)
Z	4
Calculated density (g/cm^3)	1.282
μ (mm^{-1})	0.330
Crystal shape and color	Block, colorless
Crystal size (mm)	0.28 x 0.22 x 0.14
Theta range for data collection (°)	2.067 – 26.369
Limiting indices	-11≤h ≤11, -14≤ k ≤14, -24≤ l≤24
Diffractometer	Bruker DUO APEXII CCD
Absorption correction	Multi-scan (*SADABS*, Brucker, 2012)
Tmin. Tmax.	0.6529, 0.7456
No. of measured, independent and observed [$I > 2\sigma(I)$] reflections	44491, 4766, 3838
Refinement method	Full-matrix least-squares on F^2
Data / restraints / parameters	4766/0/240
$R[F^2 > 2\sigma(F^2)]$, $wR(F^2)$, S	0.040, 0.105, 1.03
H-atom treatment	H atoms treated by a mixture of independent and constrained refinement
$\Delta\rho_{max}$, $\Delta\rho_{min}$ (e $Å^{-3}$)	0.24, -0.19
Absolute structure	Flack x determined using 1359quotients [(I+)-(I-)]/[(I+)+(I-)] (Parsons, Flack and Wagner, Acta Cryst. B69 (2013) 249-259).
Absolute structure parameter	0.005(19)

Table 5. Some selected experimental and theoretical geometric parameters for compound **2**(Å, °).

Geometric Parameters	Experimental values	DFT values
Bond (Å)		
Cl1—C1	1.771(3)	1.799
Cl2—C1	1.762(3)	1.799
O1—C8	1.242(4)	1.238
N1—C6	1.359(4)	1.366
C1—C1a	1.503(4)	1.512
C1—C9a	1.511(3)	1.523
C1a—C9a	1.536(4)	1.555
C7—C8	1.426(4)	1.452
C6—C7	1.379(4)	1.379
C14—N1	1.440(4)	1.450
Bond angles (º)		
Cl1—C1—Cl2	108.1(2)	107.92
C1—C9a—C1a	59.1(2)	58.86
C1—C1a—C9a	59.6(2)	59.51
C1—C9a—C5a	117.3(2)	117.29
C1—C1a—C2	119.5(2)	120.03
O1—C8—C7	123.1(2)	122.78
C8—C7—C6	120.6(2)	119.29
C7—C6—N1	120.2(2)	124.28
C6—N1—C14	126.6(2)	126.36
C11—C5—C12	107.4(2)	107.35

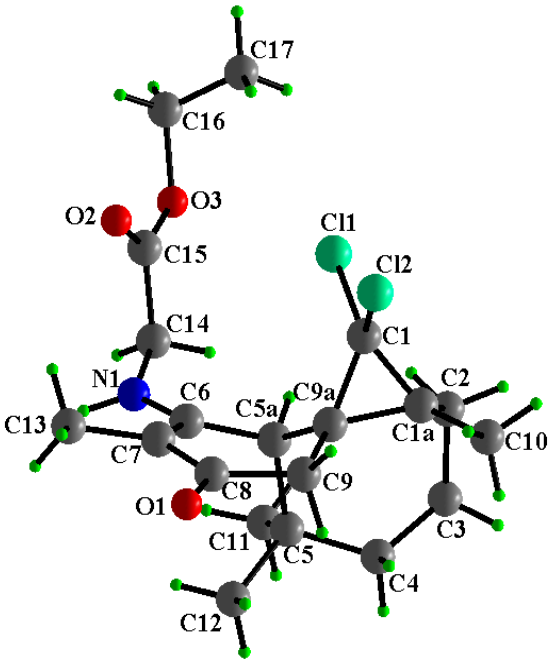

Fig. 4 Molecular view of compound **2** with the atom labeling scheme. Ellipsoids are drawn at the 50% probability level. H atoms are represented as small green circle of arbitrary radii.

In the molecule, there are three chiral carbon atoms, C1a and C5a exhibits an R configuration and C9a exhibits an S configuration. The dihedral angle between the mean planes trough the six- and seven-membered rings is 66.9(2). The three-membered ring (C1–C9a) is nearly perpendicular to the six-membered ring (C5a/C6–C9/C9a) mean plane, making a dihedral angle of 85.9(2).The six membered cycloexylidene ring have roughly screw boat conformation with the puckering parameters: Q= 0.471(3)Å, spherical polar angle θ= 61.7(4)° and φ= 322.9(4)° , whereas a puckering analysis of the seven-membered ring gave the parameters q2 = 1.148 (3) and q3 = 0.037(2), indicating it adopts a flattened boat conformation [**43**].

The C—Cl bond lengths average 1.766(3) Å, are in good agreement with the Cl---C bond length of 1.764(6) Å reported for the related compound [**44-47**]. In the amino-α- ester function, the C—N bond length range from 1.359(4) - 1.440(4) Å are similar for the structure of similar compound [**47**]. The main difference between the conformations of these molecules is observed for the cyclohexene ring (between envelope and half-chair for [**44]**, half-chair for [**45]**, screw-boat for and envelope for **[46]**.

In the crystal, molecules are linked by N—H···O and C—H···O hydrogen bonds, forming a three-dimensional framework (Fig. 5 and Table 6).There is no significant C—H···πor π–π contacts present in the crystal.

Table 6 Hydrogen bonds geometry (Å, °) for compound **2**

D—H…A	**D—H**	**H…A**	**D…A**	**D—H…A**
C3 – H3B···O2^{i}	0.97	2.44	3.395(4)	170
C10 – H10A···O1^{ii}	0.96	2.60	3.502(4)	157
N1 – H1N···O1^{iii}	0.86	2.15	2.948(3)	155

Symmetry codes: (i) – x+3/2, - y+1, z+1/2; (ii) 1 - x, 1/2 + y, 1/2- z; (iii) 1/2 + x, -1/2 - y, - z;

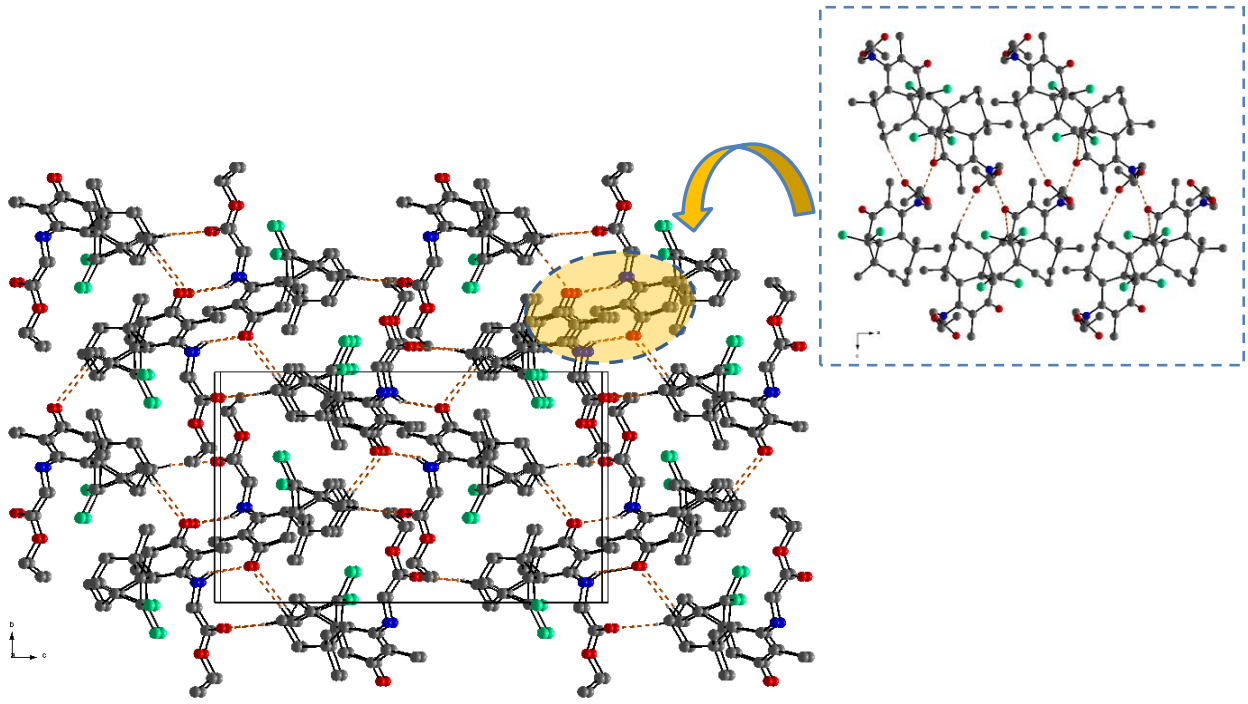

Fig 5: Packing and hydrogen-bonding interactions of the enaminone **2** viewed along the a-axis. For clarity, only the H atoms involved in the hydrogen bonds (dashed lines) interactions have been included.

Hirshfeld analysis

Hirshfeld surface (HS) analysis and two-dimensional fingerprint plots generated using *CrystalExplorer17.5* shows the various intermolecular interactions in crystal structure (Fig. 6). The positions of the strong N—H···O and C—H···O hydrogen bonds are indicated by the red regions on the Hirshfeld surface.In the view Hirshfeld surface mapped over the electrostatic potential in Fig. 7, the red and blue regions around the electronegative and electropositive atoms result from the polarization of charges about the acceptors and donors, respectively. In enaminone **2**, the most negative sites are associated with the O atom which undergoes electrophilic reactivity while the positive region over the protons of amine group indicates that these sites are susceptible for nucleophilic attack.

The two-dimensional fingerprint plots are given in (Fig. 8 a), showed the intermolecular contacts and their percentage distributions on the Hirschfeld surface. They reveal that the principal contributions to the overall surface involve H···H contacts at 61.1% (Fig. 8b),as widely scattered points of high density due to the large hydrogen content of the molecule with the tip at de = di ≈ 0.95 Å. The contribution (18.9%) from the O···H/H···O contacts shows a pair of sharp spikes corresponding to the N— H…O and C—H···O interactions (Fig. 8c). In addition, Cl···H/H···Cl and C···H/H···C contacts contribute 18.1% (Fig. 8d) and 1.7% (Fig. 8e) respectively. The large number of H···H and O···H/H···O interactions suggests that van der Waals interactions and hydrogen bonding play dominant role in stabilizing the lattice of the enaminone **2**.

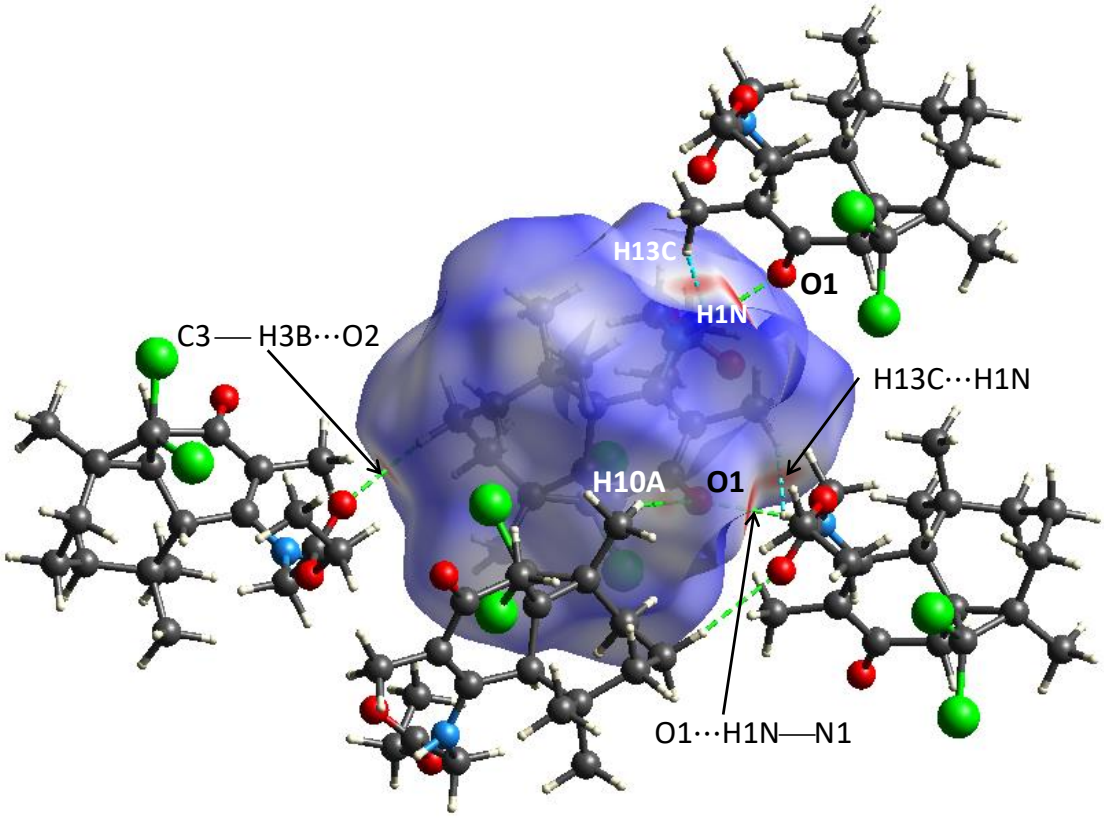

Fig.6: Hirshfeld surface of enaminone **2** mapped over d_{norm} to visualize the intermolecular interactions.

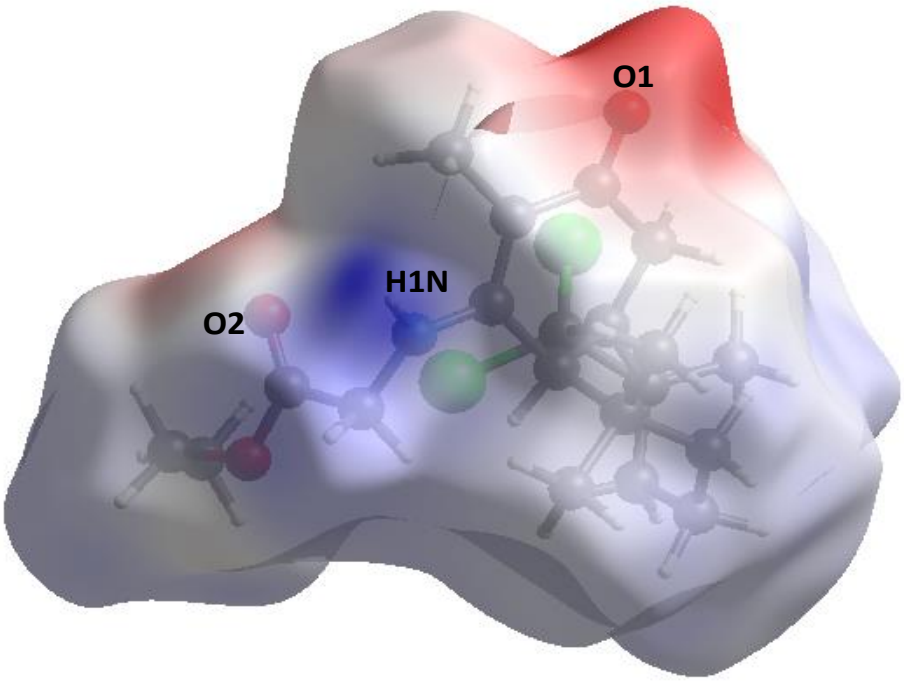

Fig. 7. Electrostatic potential mapped over the Hirshfeld surfaces of enaminone **2**

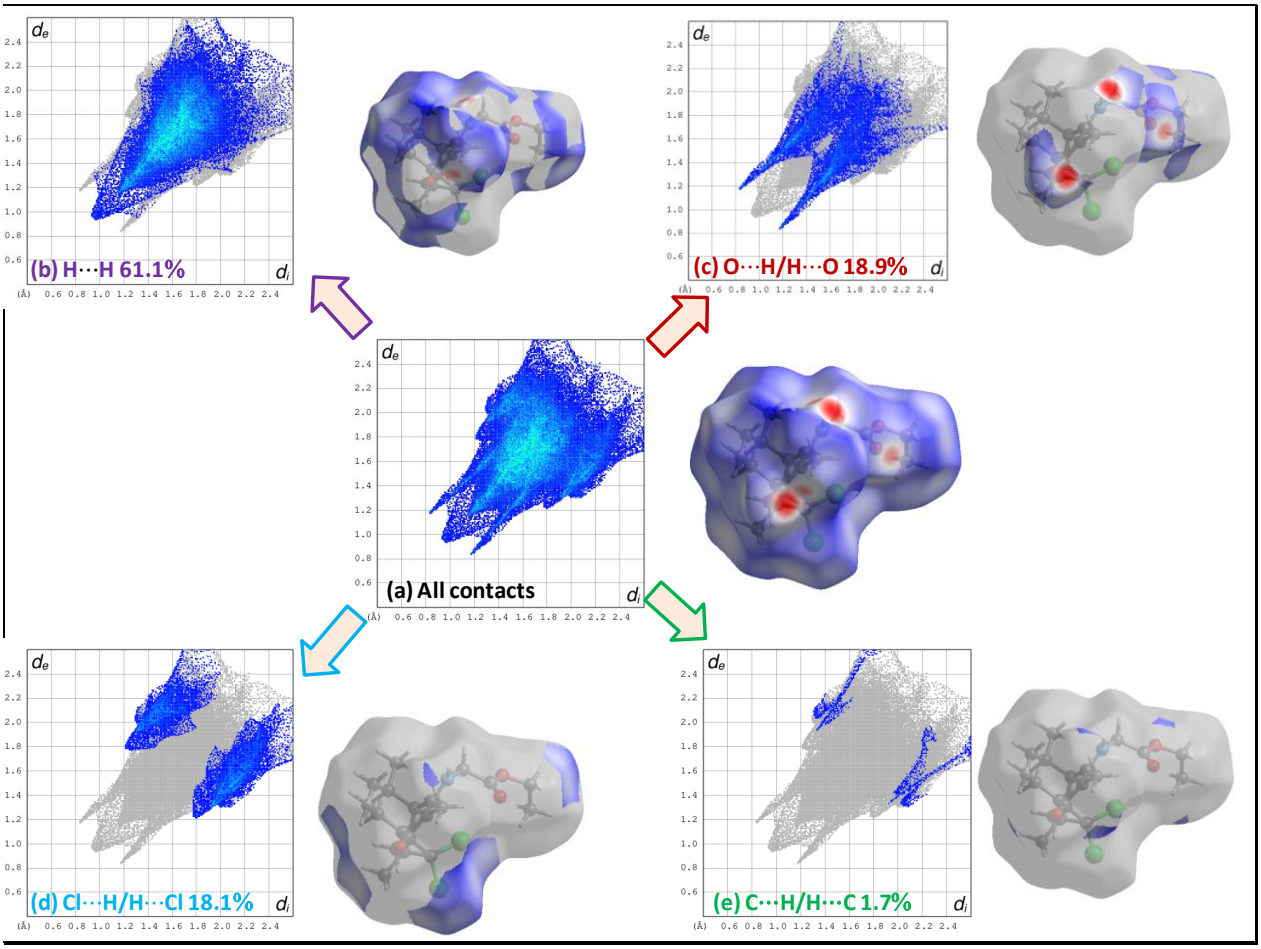

Fig. 8:(a) The two-dimensional fingerprint plots of the title compound, and delineated into (b) H···H, (c) O···H/H···O, (d) Cl···H/H···Cl and (e) C···H/H···C contacts.

Cytotoxic activity evaluation

The sesquiterpene **1** and its enaminone derivative **2** were evaluated for their cell growth inhibitory effect *in vitro* against cancer cell lines, fibrosarcoma (HT-1080), lung carcinoma (A-549) and breast adenocarcinoma (MCF-7 & MDA-MB-231)[48]. Cells were treated with different concentrations ranging from 6.25 to 100 µM during 24 hours. The topoisomerase II inhibitor doxorubicin (Dox) was used as a positive control and cell growth has been quantified using the MTS assay. Data relative to the inhibitory effect (IC_{50}) of the compounds **1** and **2** are presented in **Table 4**.

Table 4: In vitro cell growth inhibitory effect of the compounds **1** and **2.**

	IC_{50}(µM)			
Compound	**HT-1080**	**A-549**	**MCF-7**	**MDA-MB-231**
1	13.28	16.41	41.87	34.71
2	52.03	46.82	49.25	39.10
Dox	5.09	6.41	5.41	5.10

As shown in **Table 3**, the compound **1** exhibited a moderate to high antitumor activity against the four cell lines, particularly in the case of HT-1080 and MCF-7 cells. In fact, IC_{50} values in the two cell lines were respectively13.28 and 16.41 µM. However, the incorporation of enamino

function in the sesquiterpenic skeleton decreased significantly the cytotoxic effect of the compound **2**, for which IC_{50} values were ranging from 39.10 to 52.03 µM against all cell lines.

Optimized molecular structure of compound 2

The geometric structure of compound **2** was optimized using DFT at B3LYP/6-31G(d,p) level, see **Fig. 9**. The selected geometrical parameters were summarized in **Table 3**. The results in XRD and optimized geometry by DFT are almost identical and the reported deviations between both structures are due to differences in the molecular environment, which is an isolated molecule in DFT optimization and the crystalline phase in X-ray crystallography analysis. In crystalline structure, (**Fig. 9**).

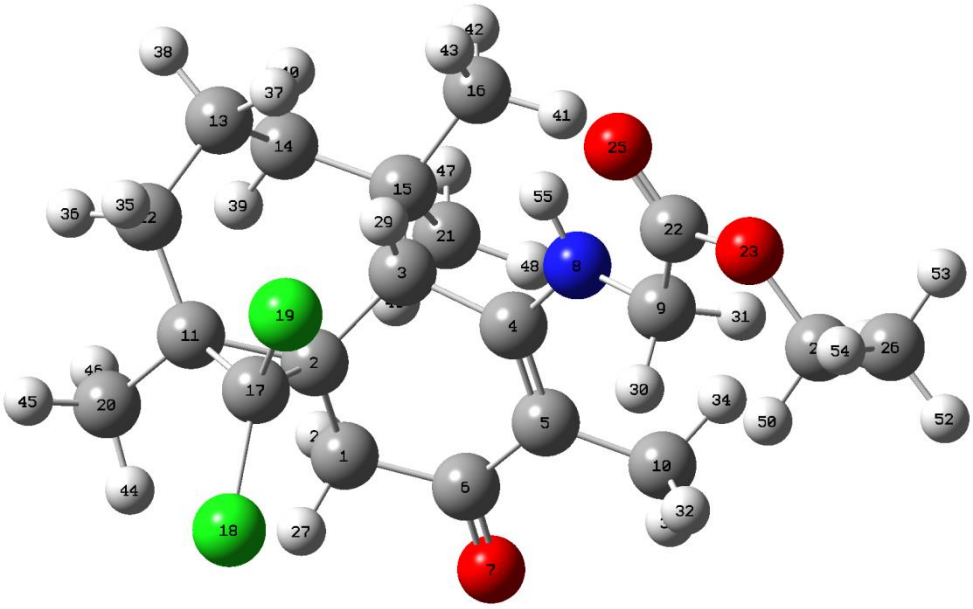

Figure 9. Optimized geometry of compound **2** at B3LYP/6-31G(d,p) level.

Mechanistic studies

In the first step for the synthesis of compound **2**, the hemachalene ketone **1** reacts with azide via 1,3-dipolar cycloaddition conducting to the formation of 1,2,3-triazole derivate (A). This step is endothermic by 11.42 kcal/mol. Then, the 1,2,3-triazole then transforms into the charged species of zwitterionic type (B) via a cleavage between the N-N band yields to the formation of an intermediate (C). The energetic barrier for this step is 25.55 kcal/mol. Finally, the formation of the product **2** derivative is exothermic by 125.48 kcal/mol. These results allow us to explain the formation of the corresponding product **2** (**Figure 10**).

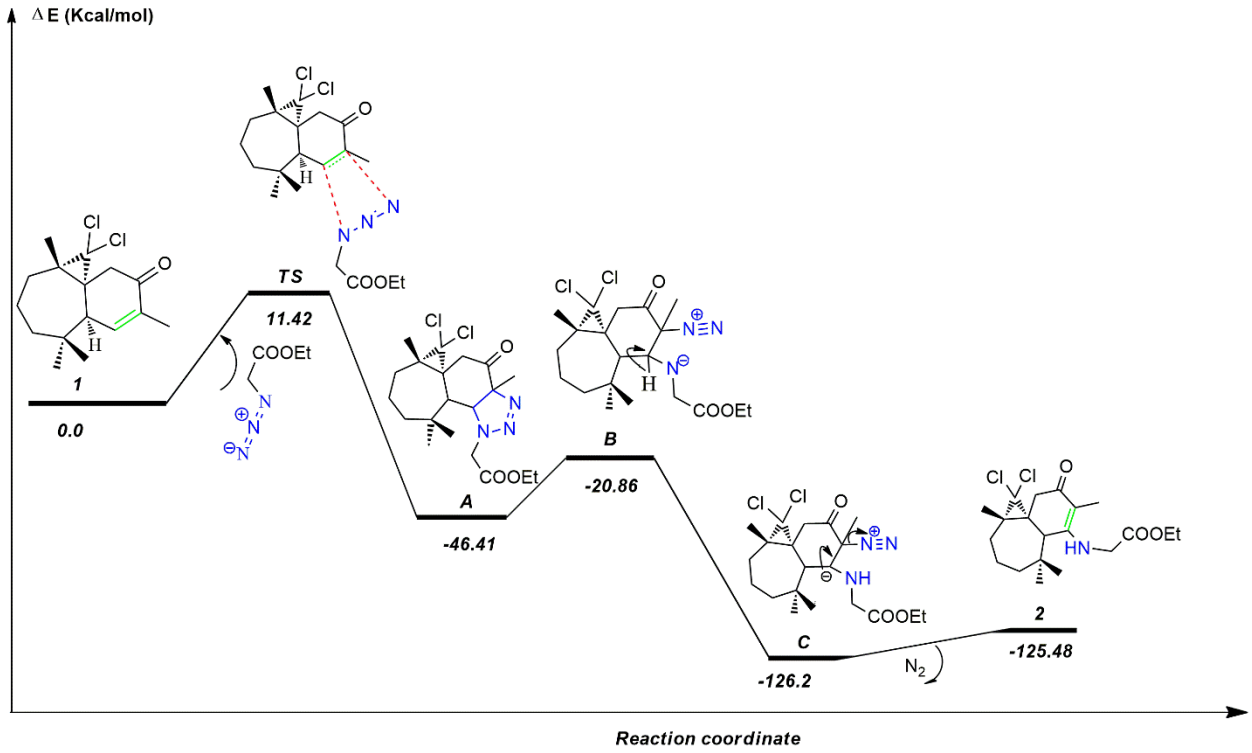

Fig.10. Proposed mechanism for the synthesis of compound **2**

Conclusion

Based on the himachalene ketone **1**, a compound, including enaminone, was synthesized using $TiCl_4$ catalyzed 1,3-dipolar cycloaddition reaction. The target compound **2** is well characterized by FT-IR, UV-Visible, NMR (^1H &^{13}C) mass spectrometry (HRMS) and also X-ray diffraction. Theoretical studies were performed on DFT/B3LYP/6-31G(d,p) level method for the purpose of comparing the spectroscopic experimental and theoretical data. The evaluation *in vitro* of the anti-proliferative activity revealed a remarkable cytotoxic effect of the compound **1**, its derivative **2**, however showed a moderate and low cytotoxic effect. In addition, the mechanism for the formation of the compound **2** was explained by the global reactivity indexes. Altogether, the theoretical results are in agreement with experimental findings.

Acknowledgements

The authors are greatly thankful to the University Cadi Ayyad for it support. The X-ray diffractometers are founded by region NPDC, FEDER, CNRS and MESR.

Supplementary materials

These data include NMR spectra for the enaminone. CCDCxxxxx contains the supplementary crystallographic data for $C_{20}H_{29}Cl_2NO_3$. These data can be obtained free of charge via www.ccdc.cam.ac.uk/data_request/cif, or by emailing data_request@ccdc.cam. ac.uk, or by contacting the Cambridge Crystallographic Data Centre, 12 Union Road, Cambridge CB2 1EZ, UK; fax: +44 1223 336033.

References

[1]. WHO Press release, (n.d.). https://www.who.int/whr/1996/media_centre/press_release/en/-index7.html (accessed November 11(2019).

[2] A. Oubella; M. Fawzi; A. Auhmani; A. Riahi; H. Morjani; A. Robert; My. Y. Ait Itto, Synthesis and Antitumor Activity of Novel Heterocyclic Systems with Monoterpenic Skeleton Combining Dichlorocyclopropane and 1,3,4-Thiadiazole Nucleus,ChemistrySelect.5 (2020) 6403–6406

[3] A. Taia, M. Essaber, A. Oubella, A. Aatif, J. Bodiguel, B. Jamart-Grégoire, My. Y. Ait Itto & H.Morjani, Synthesis, characterization and biological evaluation of new heterocyclic systems 1,2,3-triazole-isoxazoline from eugenol by the mixed condensation reactions, Synthetic Commun. 50(2020)2052-2065.

[4] A.-E. El Mansouri, A. Oubella, M. Maatallah, M.Y. AitItto, M. Zahouily, H. Morjani, H.B. Lazrek, Design, synthesis, biological evaluation and molecular docking of new uracil analogs-1,2,4-oxadiazole hybrids as potential anticancer agents, Bioorganic & Medicinal Chemistry Letters. 30 (2020) 127438.

[5] A. Oubella, My. Y. Ait Itto, A. Auhmani, A. Riahi, A. Robert, J. Daran, H. Morjani, Carol A. Parish, M. Esseffar, Diastereoselective synthesis and cytotoxic evaluation of new isoxazoles and pyrazoles with monoterpenic skeleton, Journal of Molecular Structure. 1198 (2019) 126924

[6] Z. N. Siddiqui, Bis[(L)prolinato-N,O]Zn–water: A green catalytic system for the synthesis of 3,4-dihydropyrimidin-2 (1H)-ones via the Biginelli reaction,C. R. Chimie. 16 (2013) 183–188

[7]B. A. D. Neto, A. M. Lapis, A. B. Bernd,D. Russowsky, Studies on the Eschenmoser coupling reaction and insights on its mechanism. Application in the synthesis of Norallosedamine and other alkaloids, Tetrahedron.65 (2009)2484-2496.

[8].J. Makawana, M. Patel, R. Patel,Synthesis and *in vitro* antimicrobial activity of *N*-arylquinoline derivatives bearing 2-morpholinoquinoline moiety, Chin. Chem. Lett. 23 (2012)427-430.

[9].J. E.Foster, J. M. Nicholson, R. Butcher, J. Stables, I. Edafiogho, A. M. Goodwin, M. C.Henson, C. A.Smith, K. R Scott, Synthesis, characterization and anticonvulsant activity of enaminones. Part 6: Synthesis of substituted vinylic benzamides as potential anticonvulsants,Med. Chem. 7 (1999)2415.

[10].D. Simoni, M. Rizzi, R. Rondanin, R. Baruchello, J.P. Marchetti, F. Invidiata, M. Labbozzetta, P. Poma, V. Carina, M. Notarbartolo, A. Alaimo, N. D'Alessandro. Antitumor effects of curcumin and structurally β-diketone modified analogs on multidrug resistant cancer cells, Bioorganic & Medicinal Chemistry Letters.18 (2008) 845.

[11].J. E. Foster, J. M. Nicholson, R. Butcher, J. P. Stables, I. O. Edafiogho, A. M. Goodwin, M. C. Henson, C. A. Smith, K. Scott, Synthesis, characterization and anticonvulsant activity of enaminones. Part 6: Synthesis of substituted vinylic benzamides as potential anticonvulsants, Bioorganic & medicinal chemistry.7 (11), (1999), 2415-2425.

[12] TP. Lakshmi, T. Pragna, S. Vajravijayan, M. Moumita, N. Sakthivel, K. Gunasekaran, R. Krishna, A novel guaiane sesquiterpene derivative, guai-2-en-10α-ol, from Ulva fasciata Delile inhibits EGFR/PI3K/Akt signaling and induces cytotoxicity in triple-negative breast cancer cells, Mol. Cell. Biochem. 438 (1–2) (2018) 123–139.

[13]T. Abu-Izneid, A. Rauf, M. A. Shariati, A. A. Khali, M. Imran, M. Rebezov, M. Uddin, M. F. Mahomoodally, K. R.R. Rengasamy, Sesquiterpenes and their derivatives-natural anticancer compounds: An update, Pharmacological Research. 161 (2020) 105165.

[14] Y. Ding, H. Wang, J. Niu, M. Luo, Y. Gou, L. Miao, Z. Zou, Y. Cheng, Induction of ROS overload by alantolactone prompts oxidative DNA damage and apoptosis in colorectal cancer cells, Int. J. Mol. Sci. 17 (2016) 558.

[15].D. Kumar, D. N. Kommi, P. Chopra, M. I. Ansari, A. K. Chakraborti,L-Proline-Catalyzed Activation of Methyl Ketones or Active Methylene Compounds and DMF-DMA for Syntheses of (2E)-3 Dimethylamino-2- propen-1-ones, Eur. J. Org. Chem. 2012(2012) 6407.

[16]. J. Sun, Z. P. Dong, P. Li, F. W. Zhang, S. Y. Wei, Z. Q. Shi, R. Li, Ag nanoparticles in hollow magnetic mesoporous spheres: A highly efficient and magnetically separable catalyst for synthesis of β-enaminones, Mater. Chem. Phys. 140(2013) 1.

[17].H. T. S. Braibante; M. E. F. Braibante; G. B. Rosso, D. A. Oriques, Preparation of β-enamino carbonylic compounds using microwave radiation/K-1,J. Brazil. Chem. Soc. 14(2003)1678-4790.

[18].C. A. Brandt, C. P. da Silva, C. G. Pancote, C. L. Brito, M. A. B. da Silveira,Efficient Synthetic Method for β-Enamino Esters Using Ultrasound, Synthesis.10 (2004) 1557 -1559.

[19] L. W. Xu, C. G. Xia, J. W. Li, &S. L. Zhou, Efficient Lewis base-catalyzed conjugate addition of azide ion to cyclic enones in water, Synlett. 14 (2003) 2246-2248.

[20] G.L. Milligan, C.J. Mossman, J. Aub, Intramolecular Schmidt Reactions of Alkyl Azides with Ketones: Scope and Stereochemical Studies, J. Am. Chem. SOC. 117 (1995) 10449–10459.

[21] D. Jones, A. Roberts, K. Cavell, W. Keim, U. Englert, B. W. Skelton and A. H. White, Synthesis of new adducts and co-ordination complexes of zirconium and titanium containing β-aminoketone ligands. Crystal structures of isostructural adducts MCl4·2PriHNCMe=CHCMe=O (M=Ti or Zr) and the complex [Zr(PhNCMe=CHCMe=O)$_2$Cl$_2$], J. Chem. Soc, Dalton Trans. 2 (1998) 255.

[22]W.H. Chan, G.K. Somal, C.E. Katz, H. Pei, Y. Zeng, J.T. Douglas, J. Aubé, One-Pot Synthesis of Lactams Using Domino Reactions: Combination of Schmidt Reaction with Sakurai and Aldol Reactions,J. Org. Chem. 74 (2009) 7618–7626.

[23]J. Liu, G. Cao, W. Xu, J. Cao, W. Wang, Ni(OAc)2: a highly efficient catalyst for the synthesis of enaminone and enamino ester derivatives under solvent-free conditions, Appl. Organometal. Chem, 24 (2010) 685–691.

[24]X. Duan, N. Liu, K. Liu, Y. Song, J. Wang, X. Mao, W. Xu, S. Yang, H. Li, J. Ma, Copper promoted Chan-Lam coupling between enaminones and aryl boronic acids, Tetrahedron Letters. 59 (2018) 4187–4190**.**

[25]F. Wodtke, F. R. Xavier, S. R. Mendes, A. R. M. de Oliveira, R.A. Gariani, A simple protocol for the preparation of β-enamino ketones catalyzed by NbOPO$_4$under solvent free conditions, Tetrahedron Letters. 58 (2017) 231–234.

[26] H. Eshghi, S. M. Seyedi, E. Safaei, M. Vakili, A. Farhadipour,M. Bayat-Mokhtari,Silica supported Fe(HSO4)3 as an efficient, heterogeneous and recyclable catalyst for synthesis of –enaminones and -enamino esters,J. Mol. Catal. A Chem. 364 (2012) 430–436.

[27] E.Rafiee, M. Joshaghani, S. Eavani, S. Rashidzadeh,A revision for the synthesis of β-enaminonesin solvent free conditions: efficacy of different supported heteropoly acids as active and reusable catalysts,Green Chem. 10 (2008) 982–989.

[28] A. Bimoussa, Y. Koumya, A. Abouelfida, M. Y. Ait Itto, A. Benyaich, O. Mentre, E. M. Ketatni, A. Auhmani and A. Auhmani; Hemisynthesis, crystal structure and inhibitory effect of sesquiterpenic thio-semicarbazones and thia-zolidin-4-ones on the corrosion behaviour of stainless steel in 1 M H_2SO_4 solution; Acta Cryst C75. (2019) 623-632.

[29]. A. Bimoussa, A. Auhmani, My. Y. Ait Itto, J. Daran and A. Abdelwahed; (1R,3S,8R)-3,7,7,10-Tetramethyltricyclo-[6.4.0.01,3]dodec-9-en-11-one; Acta Cryst E70. (2014). o81–o82

[**30**] *APEX2*, *SAINT* and *SADABS*. Bruker AXS Inc., Bruker (2012),.Madison, Wisconsin, USA.

[**31**] G. M. Sheldrick, SHELXT - Integrated space-group and crystal-structure determination. *Acta Crystallogr. Sect. A Found*. Crystallogr. 71 (2015) 3–8.

[**32**] G. M. Sheldrick, Crystal structure refinement with SHELXL. Acta Crystallogr. Sect. C Struct. Chem., 71 (2015).

[33] Brandenburg, Klaus, and H. Putz. "Diamond." Crystal Impact GbR, Bonn, *Germany* (2006).

[**34**] M.A. Spackman, D. Jayatilaka, Hirshfeld surface analysis. Cryst Eng Comm, 11 (2009) 19–32.

[**35**] J.J. McKinnon, D. Jayatilaka, M.A. Spackman. Towards quantitative analysis of intermolecular interactions with Hirshfeld surfaces. Chem. Commun. (2007) 3814–3816.

[**36**] M.J. Turner, J.J. McKinnon, S.K. Wolff, D.J. Grimwood, P.R. Spackman, D. Jayatilaka, M.A. Spackman, CrystalExplorer17, The University of Western Australia, (2017).

[37] G.E.. Frisch, M. J.; Trucks, G. W.; Schlegel, H. B.; Scuseria, V.. M. Robb, M. A.; Cheeseman, J. R.; Scalmani, G.; Barone, H. B.; Petersson, G. A.; Nakatsuji, H.; Caricato, M.; Li, X.; Hratchian, M.. P.; Izmaylov, A. F.; Bloino, J.; Zheng, G.; Sonnenberg, J. L.; Hada, M.. N. Ehara, M.; Toyota, K.; Fukuda, R.; Hasegawa, J.; Ishida, J..T.; Honda, Y.; Kitao, O.; Nakai, H.; Vreven, T.; Montgomery, J. A., E.N..

Peralta, J. E.; Ogliaro, F.; Bearpark, M. J.; Heyd, J.; Brothers, J..Kudin, K. N.; Staroverov, V. N.; Kobayashi, R.; Normand, S.S..Raghavachari, K.; Rendell, A. P.; Burant, J. C.; Iyengar, J.E..Tomasi, J.; Cossi, M.; Rega, N.; Millam, N. J.; Klene, M.; Knox, R.. Cross, J. B.; Bakken, V.; Adamo, C.; Jaramillo, J.; Gomperts, C..Stratmann, R. E.; Yazyev, O.; Austin, A. J.; Cammi, R.; Pomelli, V.G.. Ochterski, J. W.; Martin, R. L.; Morokuma, K.; Zakrzewski, A. Voth, G. A.; Salvador, P.; Dannenberg, J. J.; Dapprich, S.; Daniels, D.J. D.; Farkas, O.; Foresman, J. B.; Ortiz, J. V.; Cioslowski, J.; Fox, Gaussian 09, Gaussian, Inc. Wallingford, CT,. (n.d.).

[38] J. Tomasi, B. Mennucci, E. Cancès, The IEF version of the PCM solvation method: an overview of a new method addressed to study molecular solutes at the QM ab initio level, J. Mol. Struct: THEOCHEM. 464 (1999) 211–226.

[39] Alexander W. Schuppe, James M. Cabrera, Catherine L.B. McGeoch, Timothy R. Newhouse; Tetrahedron 73 (2017) 3643-3651.

[40] Zeba N. Siddiqui , Kulsum Khan, Nayeem Ahmed; Nano Fibrous Silica Sulphuric Acid as an Efficient Catalyst for the Synthesis of b-Enaminone; Catal Lett; 144 (2014) 623–632.

[41]A. Ehrhard,S. Jäger,C. Malm,S. Basaran, &J. Hunger, CF3-groups critically enhance the binding of thiourea catalysts to ketones – a NMR and FT-IR study, Journal of Molecular Liquids. (2019) 111829.

[42]B. K Oram, Monu, &B. Bandyopadhyay, Impact of donor acidity and acceptor anharmonicity on ν spectral shifts in O-H···O=C H-bonded ketone-alcohol complexes: An IR spectroscopic investigation; Spectrochimica Acta Part A: Molecular and Biomolecular Spectroscopy. 230 (2020) 118070.

[43] D. Cremer, &J. A. Pople,General definition of ring puckering coordinates. *J. Am. Chem. Soc*. 97, **(**1975)1354–1358.

[**44**] A. Auhmani, E. Kossareva, E. Lassaba, M. Réglier, M. Pierrot &A. Benharref, Réactions de cyclopropanation sur α-*cis*-himachalène et a β-himachalène,*Acta Cryst*. C55. (1999) IUC9900055.

[**45]** A. Benharref, A. Oukhrib, M. Ait Elhad, J. C. Daran and M. Berraho, *N*'-[(1S,3R,8R)-2,2-Dichloro-3,7,7,10-tetramethyltricyclo[6.4.0.0^{1,3}]dodecan-11-yl]acetohydrazide, *IUCrData*1.(2016) x160554.

[**46**] N. Ourhriss, M. Giorgi, N. Mazoir and A. Benharref, Absolute configuration and conformational disorder of a tricyclic thiosemicarbazone derivative, *Acta Cryst*. C61. (2005) o699–o701.

[**47**] A. Benharref, L. El Ammari, M. Saadi, M. Taourirte, A. Oukhrib and M. Berraho, N-[(1aR,5aR,8R,9aR)-1,1-Dichloro-1a,5,5,7-tetramethyl-1a,2,3,4,5,5a,8,9-octahydro-1H-benzo[a] cyclo propa[b][7]annulen-8-yl]acetamide, *IUCrData* 2.(2017) x170492.

[**48**] Az-E. El Mansouri, A. Oubella, A. Mehdi, My. Y.Ait Itto, M. Zahouily, H. Morjani, H. B. Lazrek. Design, synthesis, biological evaluation and molecular docking of new 1,3,4- oxadiazole homonucleosides and their double-headed analogs as antitumor agents, Bioorganic Chemistry. (2020)104558